

Unlike the situation when He is used as carrier gas, the translational and rotational temperatures are in equilibrium when using Ar. Thus in the case where 50 Torr of Ar is used as carrier, the translational and rotational temperatures are calculated to be 4.5 K and a relatively intense peak at $\Delta X_i = 0$ due to $(\text{VCl}_4)_x$ clusters is observed (figure 5). As the rotational temperature of the VCl_4 in the experiment involvi j_g 27.5 Torr of Ar is only marginally within the regime in which the Jahn-Teller motions may be frozen out and the vibrational temperature certainly will be higher still, the satellite structure observed at the expected positions in the splitting pattern (Figure 5) argue against a rapid ISR mechanism, which predicts broadening but not splitting in warm VCl_4 .

Finally, experiments carried out with Xe as carrier gave spectra much like those obtained with Kr, but with smaller signal-to-noise ratio. Satellite structure however was readily seen, in this case with a splitting larger than that observed in Kr, due to the lower velocity of the Xe beam (3.75×10^4 cm/s). This velocity leads to the expectation of satellites at ± 2.32 mm at a field of 14.4 kG, while the observed displacement is ± 2.65 mm.

The good agreement between the observed satellite spacings of VCl_4 seeded into the different rare gases and the splittings calculated on the basis of the measured velocities is possible only if the mass of the deflected species is constant in the series of experiments. Thus it is concluded that the deflected species in our beams are in no way complexed with the carrier gases. This principle of neutral-molecule mass spectrometry is useful also in identifying the species responsible for the central peak in Figure 1. Thus the possibility that the central peak is due to the mixed cluster $\text{VCl}_4\text{-Kr}$ is readily discounted, for this species is expected to have a deflection of ± 1.34 mm provided that the cluster is beyond the Paschen-Back limit so that coupling of S to rotations is irrelevant. If it is assumed that the central peak instead consists of two overlapping components with deflections of less than ± 0.1 mm and that the species responsible for these peaks is the mixed cluster $\text{VCl}_4\text{-Kr}_x$, then the small deflection amplitudes lead to $x \approx 40$ or larger.

Interpretation of the Stern-Gerlach deflection spectra of VCl_4 seeded into the heavier rare gases is reasonable assuming that the ISR processes are not important in these beams and that the spectral patterns are dictated by the coupling of a single electron spin to the external field, as influenced by beam velocity effects and by clustering to form $(\text{VCl}_4)_x$. ISR processes are insignificant here either because they do not occur in the free VCl_4 molecule or because the Jahn-Teller motions provoking ISR are frozen out in the Ar, Kr, and Xe beams. However, in the case of He as carrier gas, it is conceivable that the observed pattern is the result

of poor cooling in the beam and a concomitant ISR process, which acts to flip electron spins at a rate of $10^6/\text{s}$ or faster. What would be most illuminating at this point would be the deflection spectrum of VCl_4 vapor as an effusive beam at room temperature, for neither clustering nor static Jahn-Teller effects would be factors here, and the slow beam should show a large splitting if the molecule is free of ISR processes, but only broadening if the ISR processes are important. We have attempted this; however, the effusive beam intensity is below our sensitivity limits at the moment.

We conclude the following from these deflection experiments:

(1) Splittings within the magnetic deflection spectrum of a transition-metal compound seeded into a molecular beam of a rare-gas carrier may be seen even though the compound in the condensed phase shows very rapid spin-lattice relaxation.

(2) Under the conditions prevailing in the Ar, Kr, and Xe beams, the electron spin of the VCl_4 molecule is not being relaxed at any significant rate ($< 10^4 \text{ s}^{-1}$) by Jahn-Teller driven nuclear motions. However, the cooling in these beams is strong enough to result in the significant formation of $(\text{VCl}_4)_x$ clusters, which are either diamagnetic or weakly paramagnetic. There is no further structure observed in the splitting pattern beyond that due to electron spin, suggesting either that only $N = 0$ rotational levels are populated in the expansion or, more likely, that any possible spin-rotation coupling within VCl_4 molecules having $N > 0$ is quenched by the Paschen-Back effect at the kilogauss fields in question.

(3) The lack of VCl_4 deflection when seeded into the He beam in large part is due to the high velocity of the carrier gas; however, this does not explain the observed result quantitatively and a rapid ISR ($\tau = 10^{-6} \text{ s}$) may be a factor here. Though our results can be accommodated by the ISR theory, they must not be construed as proving the reality of this hypothesis.

(4) Any conclusive effects of ISR resulting from transitions between the Jahn-Teller minima of VCl_4 are not visible in the seeded beams used here but may appear in the deflection spectrum of an effusive beam of the compound, in which there is a low beam velocity and no complications from either clustering or cooling.

(5) Possible clustering of a paramagnetic species with the carrier gas can be ascertained by determining that the observed deflections in different carrier gases scale inversely with the squares of the measured beam velocities, for only at constant mass of the deflected particle does this inverse-square relationship hold. Alternatively, for a beam generated using any one carrier gas in which the paramagnetic molecule M and the rare gas RG combine to form $M\text{-RG}_x$ mixed clusters all moving with the same velocity, the SG deflections will scale directly with the inverse masses of the clusters.

Time-Resolved Unimolecular Dissociation of Styrene Ion. Rates and Activation Parameters

Robert C. Dunbar

Contribution from the Chemistry Department, Case Western Reserve University, Cleveland, Ohio 44106. Received October 28, 1988

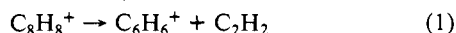
Abstract: The rate of unimolecular dissociation of styrene ion into benzene ion plus acetylene was measured by time-resolved photodissociation at 308 nm in the ICR ion trap. A rate constant of $1.10 \times 10^5 \text{ s}^{-1}$ was obtained at a total ion internal energy of 4.20 eV. Using accurate heat of formation data for the reactant and products, a 0 K reaction enthalpy of 2.42 eV was assigned. RRKM rate-energy curves were calculated for comparison with the present measurement and with previous photoionization coincidence (PEPICO) data. The shape of the RRKM curve matches experiment, and quantitative rate agreement is obtained assuming an activation energy of 2.32 eV and a tight transition state. The activation parameters derived from the activated complex, $\Delta S^\ddagger(1000 \text{ K}) = -6.4 \text{ eu}$ and $A_\ddagger(1000 \text{ K}) = 2.3 \times 10^{12} \text{ s}^{-1}$, are compared with values for other ion dissociations and with neutral-molecule rearrangements and rearrangement dissociations.

A body of precise and reliable kinetic information on the unimolecular dissociation of energy-selected low-pressure gas-phase

ions has become available through several new techniques. Moreover, the basis for making the connection and comparison

between these results and the classical understanding of the kinetics of high-pressure thermal unimolecular reactions has been established, largely through the insights of the late Henry Rosenstock and his collaborators. The styrene molecular ion, for which exceptionally extensive data are available, provides a good example of these ideas.

Understanding of the unimolecular dissociation kinetics of medium-sized polyatomics has advanced substantially through new techniques for studying fragmentations of energetically well-defined ions. Photoexcitation provides the energy control underlying two of the most precise of these methods: One of these approaches uses neutral photoionization with electron coincidence selection (PEPICO),¹ while the second involves photodissociation of thermalized ions.² A difficulty with quantitative studies of this type on ions larger than benzene is that the thermochemistry of dissociation is accurately known for few larger ion systems. Styrene ion is exceptional in this regard in that the thermochemistry of the lowest energy dissociation reaction



is known with high accuracy. This reaction is also exceptional among larger molecule systems in that there is no uncertainty about the structures of either reactant ion or products.

This dissociation reaction thus provides a well-defined opportunity for quantitative correlation of the expectations from quasi-equilibrium (RRKM) theory³ with accurate experimental kinetic data. We describe here new data from photodissociation, which is complementary to previous coincidence photoionization results, and discuss these data in light of RRKM expectations.

Smith et al.⁴ measured the rate of this reaction for several ion energies by PEPICO and concluded that RRKM theory gives a good fit to the kinetics with a transition state similar to the parent ion. In view of the substantial molecular rearrangement involved in the dissociation, one might even expect this reaction to proceed with some negative activation entropy and with a correspondingly even tighter transition state than postulated by Smith et al. To explore this question further, we have applied the recently described technique of time-resolved photodissociation in the ICR ion trap^{2,5} to confirm the experimental rate constant in the important slow-dissociation region and have reexamined the comparison with RRKM theory in light of recent thermochemical values and methods of calculation.

Experimental Section

The present experiment was similar to that described previously for time-resolved dissociation of benzonitrile ion.⁵ The principal features of the time-resolved ion-trap photodissociation experiment are (1) electron-impact formation of parent ions, (2) thermalization of the ion population by collisions and radiative cooling, (3) photoexcitation of parent ions by a 10-ns excimer laser pulse, (4) a variable time delay for unimolecular dissociation to proceed, and (5) ICR detection of the number of dissociation product ions present at the end of the delay.

In the present experiment, the styrene parent ions were thermalized for about 0.6 s at a neutral-gas pressure of $(1-2) \times 10^{-6}$ Torr, giving about 30 ion-parent neutral collisions. Since each collision with parent neutral is expected to remove a major fraction of any superthermal internal energy from the ion and since 0.6 s is comparable to the IR radiative cooling time constant of typical ions of this type,⁶ we confidently expect that the styrene parent ion population was thoroughly equilibrated with the ambient cell temperature at the time of the laser pulse. Experience with this ICR cell has suggested that (due to heating of the cell by the nearby hot filament) the effective cell temperature is about 375 K,⁵ and we will take this to be the temperature of the thermalized ions (uncertain by perhaps ± 25 K). The excimer laser pulse at 308 nm was limited by an aperture and moderately focused to a spot of the order of

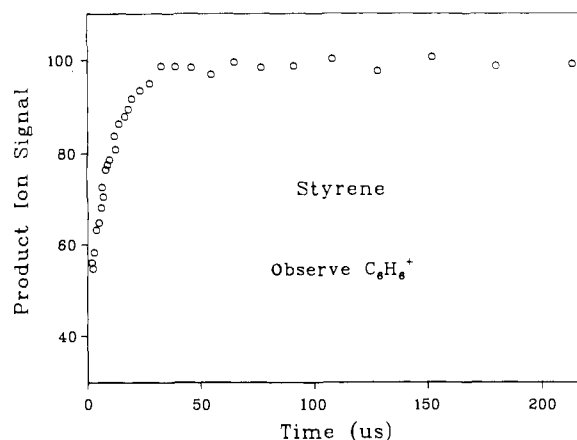


Figure 1. Time-resolved photodissociation data at 308 nm for the appearance of m/z 78 product from the unimolecular dissociation of C_8H_8^+ .

5×5 mm, giving a fluence of approximately $0.04 \text{ J}\cdot\text{cm}^{-2}$. The size of the ion cloud was comparable to or smaller than the laser spot size, based on previous experience. The photodissociation spectroscopy of styrene ion⁷ shows it to have a photodissociation cross section of about $4 \times 10^{-18} \text{ cm}^2$ at 308 nm, so a substantial extent of dissociation is expected.

Following the variable delay of 1–300 μs , an ICR excite pulse 15 μs long with 40-V peak-to-peak amplitude excited the photoproduct ions, followed by normal 2-ms ICR transient acquisition and phase-sensitive signal detection. The experimental sequence and data acquisition were automated under microcomputer control.

As reported by Wilkins and Gross,⁸ styrene ion reacts slowly with parent neutral to give m/z 130. We measured this rate approximately as $7 \times 10^{-11} \text{ cm}^3\cdot\text{molecules}^{-1}\cdot\text{s}^{-1}$, or about $1/15$ of collision rate. The 130 ion was not photoactive at 308 nm and did not interfere with the photochemistry, but since under these conditions it comprised half or more of the ions in the cell, it was ejected continuously during the time prior to the laser pulse to reduce space charge.

Data Analysis. Two complications must be considered in converting the observed product-ion production curve into a unimolecular dissociation rate constant: the thermal distribution of ion internal energies and the finite length of the ICR excite pulse. The analysis of the effect of the finite excite pulse was given in ref 2, but one modification now seems appropriate: It was assumed there that the ion cyclotron radius increases linearly with time during the excite pulse and also that the strength of the ICR signal is directly proportional to the cyclotron radius. These assumptions are valid for an infinite-parallel-plate cell but are not strictly valid in the cubical cell used, in which the radio frequency electric field and the detection sensitivity are somewhat attenuated near the cell center. A further effect, observed but not fully understood, selectively suppresses the signal of low-abundance product ions for short excite pulses; it is speculated that this arises from ion-ion interactions with the dense cloud of parent ions for product ions excited to small cyclotron radius. These nonlinearities have the effect of weighting more heavily detection of those ions formed near the beginning of the excite pulse and were approximately accounted for in eq 2 of ref 2 by reducing the parameter Δ from 15 to 10 μs .

As described in ref 2, the calculated curve was assembled by convoluting monoenergetic curves over the thermal (375 K) distribution of ion internal energies. For this convolution, the RRKM rate-energy curve shape was assumed, with the rates being multiplied by an adjustable constant to yield the calculated curve best fitting the data.

RRKM Calculations. Vibrational frequencies for the styrene parent ion were taken from Smith et al.,⁴ based on styrene neutral. One vibration at 1155 cm^{-1} was converted to the reaction coordinate. Smith et al.⁴ used the same frequencies for the transition state, but as discussed below a somewhat tighter transition state was required by the activation energy chosen here. On the basis of the rough idea that the transition state might have cyclic character in order to transfer a side-chain hydrogen to the ring, a modified frequency set was used in which two or three frequencies for loose vibrations at 416, 416, and 441 cm^{-1} were stiffened to higher frequencies. At our preferred activation energy of 2.32 eV, these three modes were set to 1100 cm^{-1} . At $E_0 = 2.42 \text{ eV}$, two of them were set to 950 cm^{-1} , and the third was left unchanged. As is well-known, the details of the frequency changes adopted are relatively

(1) Baer, T. In *Gas Phase Ion Chemistry*; Bowers, M. T., Ed.; Academic Press: New York, 1979; Vol. 1, Chapter 5; *Adv. Chem. Phys.* **1986**, *64*, 111.

(2) Dunbar, R. C. *J. Phys. Chem.* **1987**, *91*, 2801.

(3) Forst, W. *Theory of Unimolecular Reactions*; Academic Press, New York, 1973. Robinson, P. J., Holbrook, K. A. *Unimolecular Reactions*; Wiley-Interscience, New York, 1972.

(4) Smith, D.; Baer, T.; Willett, G. D.; Ormerod, R. C. *Int. J. Mass Spectrom. Ion Processes* **1979**, *30*, 155.

(5) So, H. Y.; Dunbar, R. C. *J. Am. Chem. Soc.* **1988**, *110*, 3080.

(6) Dunbar, R. C.; Chen, J. H.; So, H. Y.; Asamoto, B. *J. Chem. Phys.* **1987**, *86*, 2081.

(7) Fu, E. W.; Dunbar, R. C. *J. Am. Chem. Soc.* **1978**, *100*, 2283. Dunbar, R. C.; Kim, M. S.; Olah, G. A. *J. Am. Chem. Soc.* **1979**, *101*, 1368.

(8) Wilkins, C. W.; Gross, M. L. *J. Am. Chem. Soc.* **1971**, *93*, 895.

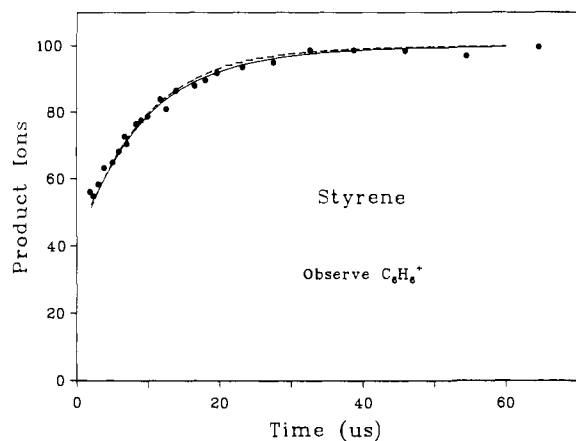


Figure 2. Initial portion of the data from Figure 1 with RRKM fits. The solid line is the calculated RRKM curve using the transition state discussed in the text, convoluted over a thermal distribution of ion internal energies at 375 K. The dashed curve is calculated using a single unimolecular rate constant of $1.10 \times 10^5 \text{ s}^{-1}$.

unimportant, with only the resulting ΔS^\ddagger value being very significant.

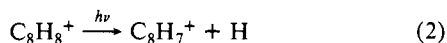
Vibrational state densities were calculated with the steepest descents approximation.⁹ For molecules as large as this (state densities here are of the order of $10^{19}/\text{cm}^{-1}$), the steepest descents approximation is the method of choice, since its accuracy and reliability, already good for small systems, become steadily better as the molecule becomes larger. No correction was made for adiabatic rotations, since the moments of inertia of our (vaguely defined) tight transition state are not obviously different from those of the energized molecule. A symmetry factor of unity was used.

Results and Discussion

Figure 1 shows data over the range of time delays from 1 to 300 μs . The ions were completely collision free over this time, as proven by the duration of the ICR transient. The daughter-ion signal remained level to beyond 1000 μs , but at delay times longer than a few milliseconds the effect of ion-molecule reactions on the product ion abundance began to appear, probably reflecting a laser-induced pressure burst in the cell.

In Figure 2 the short-time data are replotted on an expanded time scale, along with the calculated curve fitted to the data as discussed above. The best fit was obtained by assigning a rate constant of 1.10×10^5 at an ion internal energy of 4.20 eV.

Dissociation Products. As expected the major product was m/z 78 (eq 1), but a significant amount of m/z 103 was also formed:



The abundance ratio of 78 to 103 was about 3 to 1. m/z 103 is reported as only 0.3 eV higher in appearance potential than 78¹⁰ and may be formed with a much higher frequency factor, so its appearance in competition with 78 at an internal energy 1.6 eV above threshold would not be surprising. Taking such a competition into account would lead to some modest modification of the activation parameters derived below for reaction 1,¹¹ but since

(9) Forst, W.; Prasil, Z. *J. Chem. Phys.* **1969**, *51*, 3006.

(10) Lifshitz, C.; Goldberg, M.; Malinovich, Y.; Peres, M. *Int. J. Mass Spectrom. Ion Processes* **1983**, *46*, 269.

(11) If m/z 103 is indeed formed in competition with 78, there are important consequences for the interpretation of observed fragmentation rates. The observed rate constant for parent-ion disappearance and the observed rate constants for appearance of 103 and 78 will all reflect the sum of the unimolecular rates of the two fragmentation channels. Thus for comparison with RRKM modeling of the individual rate for the 78 channel, the observed rate at each internal energy should be corrected by subtracting the contribution of the 103 channel. At the 4.20 eV of the present experiment, this would mean lowering the rate by about 25%. The appropriate corrections at the higher energies of Smith et al. are unknown. If the branching ratio is fairly constant over the energy range considered here, then the effect of making this correction would be to lower the frequency factor derived in the text by 25%, which is fairly insignificant. If, as seems likely, the contribution of the 103 channel increases with energy, the appropriate corrections would also have the result of lowering (by an unknown amount) the activation energy derived from the slope of the rate-energy curve.

Table I. Thermochemical Values^a

	0 K ^b	298 K
$\Delta H_f^\circ(\text{C}_8\text{H}_8^+)$, kJ/mol	980	962
$\Delta H_f^\circ(\text{C}_6\text{H}_6^+)$, kJ/mol	986	975
$\Delta H_f^\circ(\text{C}_2\text{H}_2)$, kJ/mol	227.3	226.7
ΔH_{rx}° , kJ/mol (eV)	233.3 (2.42)	240 (2.49)
IE(C_8H_8), eV		8.42

^a Values not otherwise referenced are from ref 12. ^b Derived from 298 K values by standard statistical mechanical corrections.

it is by no means certain that the two product channels are in statistical competition and sufficient data do not yet exist to make the appropriate corrections, no attempt will be made to allow for this.

The m/z 103 signal appeared with no observable delay after the laser pulse, but reflection shows that this lack of time dependence of the product-ion signal tells little about the actual rate of ion formation:

The use of ICR to observe the time dependence of parent ion fragmentation depends on the assumption that any parent ion that fragments *after* the ICR excite pulse will give no ICR signal at the daughter-ion frequency. This is normally true if parent and daughter differ substantially in cyclotron frequency, first because the ICR excite pulse at the daughter frequency does not excite parent ions and second because parent- and daughter-ion cyclotron orbits have rapidly varying relative phase during the dissociation period. This assumption breaks down, however, if the parent and daughter ions are too close together in mass. In this case the excite pulse (if it is short enough) excites the parent ions as well as the daughter ions. If the parents then dissociate before the parent- and daughter-ion cyclotron motions have time to fall out of phase, the new daughter ions will be formed with phase-coherent cyclotron excitation and will give a signal just as if they had been formed *before* the excite pulse.

These arguments will be given in quantitative detail in a future publication; the result is that no daughter-ion time dependence will be seen if both the excite pulse and also the parent-ion dissociation time constant are rapid compared with the parent/daughter dephasing time, $(\omega_d - \omega_p)^{-1}$, where ω_d and ω_p are the respective angular cyclotron frequencies of parent and daughter ions. These requirements are met for the m/z 104/103 parent/daughter pair of eq (2) at dissociation rates faster than about 10^4 s^{-1} . It is likely that the appearance rate of m/z 103 is the same as the $1.10 \times 10^5 \text{ s}^{-1}$ of m/z 78, in which case no time dependence of the m/z 103 signal would be expected, in agreement with the experimental result.

The extent of dissociation (at long delay times) was of the order of 20–30%. This makes it likely that about a quarter of the photoexcited ions were excited sequentially by two or more photons, but we believe that the two-photon ions were not significant in these results. First, the 78 and 103 product ion signals showed identical, linear dependence on light intensity, extending to more than 50% parent-ion dissociation. Second, we expect that following photoexcitation by two photons to an internal energy of about 8 eV a parent ion will either dissociate extremely rapidly to C_6H_6^+ or dissociate to other, more endothermic product ions. The first of these possibilities would be signaled by a variation with light intensity in the zero-time intercept of the product-ion appearance curve. However, careful comparison showed no change in the curve shape for a factor of 2 difference in light intensity. Apparently any two-photon excitations that occur lead to other fragment ions. No other smaller photofragments attributable to this process were found, but this is not surprising since the very large internal energy of two photons (8 eV) might be expected to break the molecule into numerous low-abundance products, no one of which would necessarily be observable at our modest sensitivity.

Thermochemistry. The heats of formation of all three of the species in eq 1 are accurately known, leading to a very reliable value for the adiabatic endothermicity of the dissociation. The ionization energy of styrene at 298 K has been accurately measured,¹² giving a good $\Delta H_f^\circ_{298}(\text{C}_6\text{H}_6^+)$ value. Similarly, $\Delta H_f^\circ_{298}(\text{C}_8\text{H}_8^+)$

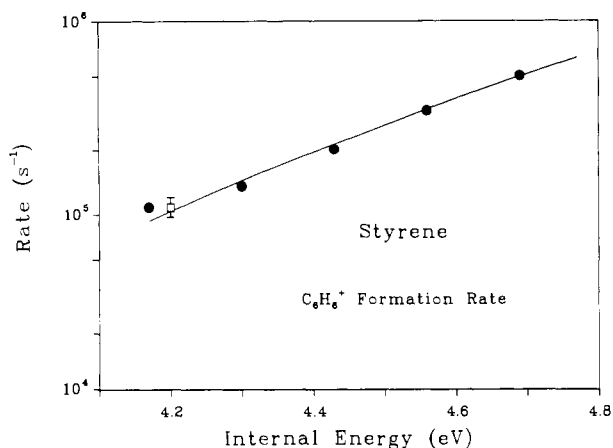


Figure 3. Quantitative rate–energy information for the styrene ion dissociation: (●) Smith et al.'s⁴ photoionization coincidence values; (□) the value from the present work. The solid curve is the RRKM curve calculated as described in the text with a tight transition state and $E_0 = 2.32$ eV.

is accurately known from the ionization energy of benzene.¹² These values may be converted to ΔH_f° values by routine corrections for heat capacities (using vibrational mode frequencies of the neutral molecules), and the relevant enthalpies are listed in Table I. The resulting thermochemical enthalpies of dissociation at 298 K and at 0 K are tabulated and should not carry an uncertainty much greater than ± 3 kJ/mol, or ± 0.3 eV. The $\Delta E(0\text{ K})$ value of 2.42 eV is the E_0 value which would be appropriate for a completely loose transition state in the RRKM calculation.

An experimental upper limit for the reaction endothermicity can be derived from the difference between the appearance energy of C_6H_6^+ and the ionization energy of C_8H_8^+ . Because of the inherent uncertainties in appearance energy measurements this is much less reliable for assigning the reaction endothermicity than the adiabatic value calculated above from the heats of formation, but it is still interesting to note this value for comparison. The value least subject to kinetic shift is the ion-trap photoionization measurement of Lifshitz,¹⁰ which gave 2.68 eV for the dissociation threshold. This is noticeably higher than the adiabatic value from heats of formation, but the discrepancy should not be considered too seriously, because the kinetic shift at 2-ms detection time may still be tenths of an electronvolt, based on RRKM modeling.

Rate Constants and Activation Parameters. As is seen in Figure 3, the present determination by photodissociation is in excellent accord with Smith et al.'s PEPICO result. Since the slow dissociation at this energy is near the limit of their technique, it is very reassuring that these two very different measurements agree.

It will be most useful to consider both the magnitude of the dissociation rates and the shape of the rate–energy curve, within the context of RRKM theory.⁴ RRKM calculation for the reaction depends on assigning a critical energy E_0 and a frequency factor; these two quantities compensate in that they can be increased or decreased together by quite large amounts without large changes in the resulting rate–energy curve. For a simple bond-breaking ion dissociation, with a very loose transition state, the critical energy should be close to the reaction endothermicity, but in the present case involving extensive rearrangement and a tight transition state this is an unreliable approach to assigning E_0 .

As a second possibility for finding E_0 , the slope of the rate–energy curve depends on E_0 , allowing E_0 to be found directly from rate data over a wide enough energy range. This possibility is explored in Figure 4, where three different E_0 values have been used with appropriate frequency factors to fit the data. The middle value, 2.42 eV, is equal to ΔE , the (0 K) endoergicity of the reaction; the value of 2.52 eV shows the effect of a significant additional activation barrier and is close to the value (2.51) as-

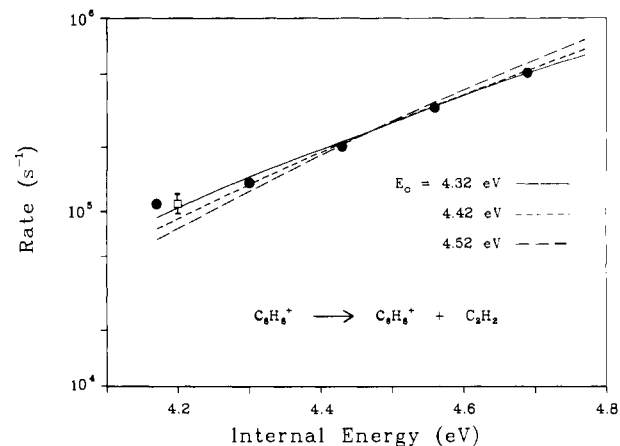


Figure 4. Data as in Figure 3, showing the RRKM fit with the preferred activation parameters of $E_0 = 2.32$ eV and $\Delta S^\ddagger = -6.4$ eu, compared with the RRKM calculations with E_0 values of 2.42 and 2.52 eV (dashed curves).

sumed by Smith et al.; while 2.32 eV is the value we choose as giving the best fit. It can be seen that the two lower values give reasonable agreement with experiment, while the 2.52-eV curve is a bit outside of a reasonable fit. Thus we assign E_0 as 2.32 ± 0.1 eV; it would require data over a much wider energy range to specify E_0 more closely than this based on the slope of the curve.

While it may seem surprising to assign the value of E_0 less than the reaction endothermicity, this is in fact entirely reasonable. The ideas of multiple transition states and transition-state switching, elaborated for ionic systems by Chesnavich, Bass, Su, Jarrold, Bowers, and others of their colleagues,^{13–16} suggest that, in addition to an orbiting transition state, a typical ion dissociation will have at least one additional transition state lying closer to reactants. The reaction rate will be governed by the transition state having the lowest flux, which for ion energies substantially above threshold will normally be an inner transition state. The inner transition state may easily have a critical energy E_0 below the reaction endoergicity ΔE and still be rate limiting at a given ion energy, since the reactive flux across each transition state depends both on its activation energy and on its activation entropy. For instance, in modeling dissociations of C_4H_6^+ and C_4H_8^+ , a number of rate-limiting transition states were assigned activation energies well below the corresponding orbiting complexes. At the high ion energies of the present case, there is thus nothing surprising about postulating a rate-limiting tight complex with E_0 below the reaction endoergicity. More complex mechanisms, such as proton transfer within a loose orbiting complex,¹⁷ lead to similar possibilities.

Further information about the dissociation potential surface comes from kinetic energy release. An activation barrier in excess of ΔE , the reaction endoergicity, may be reflected in a release of excess kinetic energy in the dissociation, as the separating fragments drop off the potential barrier. It is expected that much of the extra barrier energy (reverse activation energy) will appear as product–ion translation (although this is not assured if the high-energy transition state lies far from the product geometry).

The expected kinetic energy release for the styrene ion reaction can be estimated either from the RRKM calculation or from the equation of Klots,¹⁸ either of which gives a predicted average kinetic energy of about 100 meV for metastable ion fragmentation on a time scale of 10 μs (assuming no reverse activation energy).

(13) Jarrold, M. F.; Bass, L. M.; Kemper, P. R.; van Koppen, P. A. M.; Bowers, M. T. *J. Chem. Phys.* **1983**, *78*, 3756.

(14) Chesnavich, W. J.; Bass, L.; Su, T.; Bowers, M. T. *J. Chem. Phys.* **1981**, *74*, 2223.

(15) Bowers, M. T.; Jarrold, M. F.; Wagner-Redeker, W.; Kemper, P. R.; Bass, L. M. *Faraday Discuss. Chem. Soc.* **1983**, *75*, 57.

(16) Chesnavich, W. J.; Bowers, M. T. *Prog. React. Kinet.* **1982**, *11*, 137.

(17) As, for instance, in: Hudson, C. E.; McAdoo, D. J. *Int. J. Mass Spectrom. Ion Processes* **1984**, *59*, 325.

(18) Klots, C. E. *Adv. Mass Spectrom.* **1974**, *6*, 969.

(12) Rosenstock, H. M.; Draxl, K.; Steiner, B. W.; Herron, J. T. *J. Phys. Chem. Ref. Data, Suppl.* **1977**, *6*.

Table II. Activation Parameters for Several Transition-State Models^a

E_0^b	$\Delta S^\ddagger(1000)^c$	$A_\infty(1000)^d$	E_0^b	$\Delta S^\ddagger(1000)^c$	$A_\infty(1000)^d$
2.32	-6.4	2.3×10^{12}	2.52	-1.7	2.4×10^{13}
2.42	-4.3	6.7×10^{12}			

^aRate-energy curves for these three models are plotted in Figure 4. ^bRRKM critical energy (eV). ^cActivation entropy at 1000 K [eu (cal·K⁻¹)]. ^dFrequency factor at 1000 K (s⁻¹).

The kinetic energy release has been measured several times for metastable ion decomposition¹⁹ and is about 140 meV. This excess above the predicted value is so small as to have little significance, indicating that the reaction proceeds with little or no reverse activation energy and gives an added indication that the rate-limiting transition state lies near or below the ΔE value of 2.42 eV.

Having assigned E_0 , we can readily assign a set of activated complex vibrational frequencies to give a rate-energy curve fitting the data, as shown in Figure 3. It is seen that the experimental rate-energy curve is in excellent accord with the expected RRKM shape over the range from 1 to 6×10^5 s⁻¹, and we concur fully with Smith et al.'s conclusion⁴ that statistical theory gives an excellent description of this reaction.

An illuminating approach to viewing such ion-dissociation data and comparing different systems, suggested by Rosenstock,²⁰ is to use the RRKM activated complex parameters to write the rate of the hypothetical thermal decomposition of the ion in the high-pressure limit at the standard temperature of 1000 K. Where the microcanonical rate-energy curve has been measured directly, as in the present case, this calculation can be done with confidence within the validity of activated complex rate theory for the unimolecular reaction in question. Our preferred activated complex parameters give $\Delta S^\ddagger(1000) = -6.4$ eu and $A_\infty(1000) = 2.3 \times 10^{12}$ s⁻¹. The corresponding values for the other sets of activation parameters of Figure 4 are summarized in Table II.

Activation parameters for a number of ion fragmentations have been reported, several of which are tabulated in Lifshitz's recent review.²¹ Among rearrangement dissociations, several are of interest for comparison with the present results. Two other ions studied directly by energy-resolved methods, 4-bromotoluene²² and *tert*-butylbenzene,²³ gave ΔS^\ddagger values of -4.85 and -11.0 eu, which are quite comparable to the present -6.4 eu for styrene ion. Several values derived from less direct crossover analysis include phenol ion (+2.2 eu)²⁴ and tropone ion (-0.7 eu),²⁵ which are

reasonable for fairly tight transition states, and anisole (+7.25 eu),²⁶ which seems unreasonably high for a rearrangement, and may repay further measurement and interpretation. Also from crossover analysis,²⁷ benzonitrile ion was reported at +0.4 eu (with a previous more positive ΔS^\ddagger being apparently wrong²⁸). In contrast, simple bond cleavage dissociations of ions have been reported with positive ΔS^\ddagger values between 2.7 and 8 eu.

Activation parameters for rearrangements and rearrangement fragmentations of neutrals span a wide range of values^{3,29} but support the generalization that most log A_∞ values lie between 11 and 14, corresponding roughly to ΔS^\ddagger between -12 and +2 eu. The range of values noted above for ion dissociations is thus entirely compatible with neutral values (with the exception of anisole ion).

As indicated by Table II, the choice of E_0 for this reaction affects the derived entropy of activation, but even the high E_0 value of 2.52 eV puts $\Delta S^\ddagger(1000)$ noticeably negative, reflecting quite a tight activated complex, which is reassuring for this rearrangement dissociation. The activated complex parameters assigned by Smith et al. correspond to $\Delta S^\ddagger(1000) = -1.2$ eu, $A_\infty(1000) = 3.1 \times 10^{13}$ s⁻¹.

Assessment of the Monoenergetic Approximation for Thermal Ions. For simplicity of analysis of dissociation rate results it would be very attractive to avoid the convolution over the thermal energy distribution of the ions. It would be simplest to assign to all the ions an internal energy equal to the average internal energy and calculate the dissociation curves on this basis (as, for instance, Smith et al. did in deriving the points plotted in Figure 3). The present results give an excellent opportunity to test the extent of error introduced by this simplification. As described above, Figure 2 shows the curve calculated by convoluting the RRKM rate-energy curve over the 375 K thermal distribution. Also shown on Figure 2 is a curve fitted to the data assuming a single rate of 1.10×10^5 s⁻¹ for all ions, which is the rate for ions at 0.17-eV excess internal energy (the average thermal energy at 375 K). The two curves are practically coincident, the exact thermal curve giving a slightly better fit at long times. We conclude that the assumption of a uniform internal energy for all the ions, equal to the average thermal energy, gives almost as good a fit to the data as the exact fit and is a fully acceptable approximation.

Acknowledgment. The support of the National Science Foundation and of the donors of the Petroleum Research Fund, administered by the American Chemical Society, is gratefully acknowledged. We thank Prof. John Holmes for access to his extensive metastable-ion data base.

(19) Jones, E. G.; Beynon, J. H.; Cooks, R. G. *J. Chem. Phys.* **1972**, *57*, 2652. Gross, M. L.; DeRoos, F. L. *J. Am. Chem. Soc.* **1976**, *98*, 7128. Lifshitz, C.; Eaton, P. *Int. J. Mass Spectrom. Ion Phys.* **1983**, *49*, 337.

(20) Rosenstock, H. M.; Stockbauer, R.; Parr, A. C. *J. Chem. Phys.* **1979**, *71*, 3708.

(21) Lifshitz, C. *Adv. Mass Spectrom.*, in Press.

(22) Baer, T.; et al., to be submitted for publication.

(23) Baer, T.; Dutuit, O.; Mestdagh, H.; Rolando, C. *J. Phys. Chem.*, in press.

(24) Malinovich, Y.; Lifshitz, C. *J. Phys. Chem.* **1986**, *90*, 4311.

(25) Ziesel, J. P.; Malinovich, Y.; Ohmichi, N.; Lifshitz, C. *Chem. Phys. Lett.* **1987**, *136*, 81.

(26) Ziesel, J. P.; Lifshitz, C. *Chem. Phys.* **1987**, *117*, 227.

(27) Rosenstock, H. M.; Stockbauer, R.; Parr, A. C. *J. Chim. Phys. Phys-Chim. Biol.* **1980**, *77*, 745.

(28) Chesnavich, W. J.; Bowers, M. T. *J. Am. Chem. Soc.* **1977**, *99*, 1705.

(29) Benson, S. W. *Thermochemical Kinetics*; Wiley-Interscience, New York, 1976.